

# Crystal structure and solution-state study of $K[Al(mal)_2(H_2O)_2] \cdot 2H_2O$ ( $H_2mal = malonic acid$ )<sup>†</sup>

Andrea Tapparo,<sup>\*a</sup> Sarah L. Heath,<sup>b</sup> Peter A. Jordan,<sup>b</sup> Geoffrey R. Moore<sup>b</sup> and Annie K. Powell<sup>b</sup>

<sup>a</sup> *Università degli Studi di Padova, Dipartimento di Chimica Inorganica, Metallorganica ed Analitica, via Marzolo 1, 35131 - Padova, Italy*

<sup>b</sup> *School of Chemical Sciences, University of East Anglia, Norwich NR4 7TJ, UK*

The new complex  $K[Al(mal)_2(H_2O)_2] \cdot 2H_2O$  [ $H_2mal = CH_2(CO_2H)_2$ ] has been synthesized and its crystal structure determined by X-ray crystallography. An investigation of metal speciation in aqueous solution (analytical concentration around  $50 \text{ mmol dm}^{-3}$ ) by using  $^{27}Al$ ,  $^1H$  and  $^{13}C$  NMR spectroscopies revealed that, in solutions at physiological pH (7.5), the bis(malonate) complex evolves to the tris(malonate),  $[Al(mal)_3]^{3-}$ , without precipitation of aluminium hydroxide.

Aluminium compounds have been used extensively in both *in vivo* and *in vitro* toxicological experiments,<sup>2</sup> with the aim of developing toxicological models for the study of aluminium-related pathologies, including Alzheimers disease,<sup>3,4</sup> dialysis encephalopathy<sup>5</sup> and iron-adequate microcytic anaemia.<sup>6</sup>

In order to avoid aluminium hydroxide precipitation in solutions kept at physiological pH (around neutrality), several aluminium complexes [citrate, tartrate, gluconate, lactate, acetylacetonate, maltolate (3-hydroxy-2-methyl-4H-pyran-4-onate)] have been utilized in experimental toxicology<sup>1,7</sup> and, in general, a marked speciation effect has been observed. These observations underline the role played by small biomolecules in co-ordinating and transporting metal ions in biological systems and, in the case of aluminium, they stress the fundamental concept of metal speciation in the setting up of well defined toxicological protocols. Thus, it is important to determine both solid- and solution-state structures in order to identify potentially toxic species.

In previous papers of this series<sup>1,8,9</sup> the preparations of  $[Al_2(cit)_2(H_2O)_6]$ ,  $[Al_2(tart)_3(H_2O)_4]$ ,  $[Al(gluc)(OH)_2]$  and  $[Al(lact)_3][H_3cit = citric \text{ acid } (2\text{-hydroxypropane-1,2,3-tricarboxylic acid}), H_2tart = tartaric \text{ acid}, Hgluc = gluconic \text{ acid} \text{ and } Hlact = lactic \text{ acid}]$  have been described together with their solution-state behaviour. Crystallographic data could only be obtained on the  $[Al(lact)_3]$  complex.<sup>8</sup>

The aluminium-malonic acid ( $H_2mal$ ) system has been recently studied by potentiometry<sup>10</sup> and therefore thermodynamic data on the relevant species are available. Spectroscopic investigations of the system, using  $^{27}Al$  and  $^{17}O$  NMR, on solutions prepared by dissolving a soluble aluminium salt (sulfate or nitrate) and malonic acid, have been reported by Greenaway<sup>11</sup> and Venema *et al.*<sup>12</sup> respectively and a  $^{13}C$  NMR study on a better defined aluminium malonate complex has been reported by Amirhaeri *et al.*,<sup>13</sup> however these gave little clear information on the speciation of aluminium-malonate complexes in solution. In this paper we report on the synthesis, characterization, crystal structure and solution-state characteristics of  $K[Al(mal)_2(H_2O)_2] \cdot 2H_2O$ .

## Experimental

### Instrumentation

The infrared spectrum was recorded on a Mattson Galaxy spectrometer from  $4000$  to  $400 \text{ cm}^{-1}$  with 16 scans and a

resolution of  $4 \text{ cm}^{-1}$ ,  $^{27}Al$  NMR spectra using a JEOL GX400 spectrometer and  $^1H$  and  $^{13}C$  NMR spectra using a Bruker AC 200 FT spectrometer at  $25^\circ C$ . For the  $^{27}Al$  NMR spectra the  $[Al(H_2O)_6]^{3+}$  signal was used as the external standard. Proton and  $^{13}C$  chemical shifts were referenced to sodium 3-(trimethylsilyl)propanoate (Sigma). Instrumental conditions are given in the figure captions. Except for the experiments described in Fig. 8 (see Discussion) all solutions were prepared by dissolving the synthesized complex to give a  $50 \text{ mmol dm}^{-3}$  solution in deuterium oxide (Sigma, 99.9%). To avoid irreversible precipitation of aluminium hydroxide the pH was gradually adjusted by addition of diluted solutions (*ca.* 2%) of sodium deuterium oxide or deuterium chloride, prepared from 40% NaOD and 20% DCl solutions, respectively (Aldrich). A Crison 2002 pH meter, equipped with an Ingold micro-combined glass electrode, was used and calibrated daily using two standard buffer solutions (Radiometer, pH 7.00 and 4.01). The pH-meter response was converted using the equation  $pD = pH + 0.45$  for the deuterium oxide solutions.<sup>14</sup>

### Synthesis of $K[Al(mal)_2(H_2O)_2] \cdot 2H_2O$

The salt  $Al(NO_3)_3 \cdot 9H_2O$  (1 mmol, Sigma), malonic acid (3 mmol, Sigma) and potassium hydroxide (6 mmol) were dissolved in distilled water ( $30 \text{ cm}^3$ ). The pH was *ca.* 3.5. The complex  $K[Al(mal)_2(H_2O)_2] \cdot 2H_2O$  was obtained as a microcrystalline powder upon addition of dimethylformamide ( $20 \text{ cm}^3$ ) and letting this solution stand at room temperature for 1 week (yield *ca.* 60%). Suitable crystals for X-ray diffraction studies were prepared by dissolving 150 mg of the microcrystalline powder in water ( $5 \text{ cm}^3$ ), adding dimethylformamide ( $5 \text{ cm}^3$ ) and letting this solution stand at room temperature. The elemental analysis of the crystals, dried under vacuum at room temperature, was satisfactory (Found: C, 21.30; H, 3.45; Al, 7.60. Calc: C, 21.05; H, 3.55; Al, 7.90%).

### X-Ray crystallography

A white block crystal of  $K[Al(mal)_2(H_2O)_2] \cdot 2H_2O$  having dimensions of  $0.30 \times 0.30 \times 0.25 \text{ mm}$  was mounted on a glass fibre. All measurements were made on a Nicolet-Siemens R3mV single-crystal diffractometer system equipped with a sealed-tube molybdenum source controlled by a MicroVAX 3100 computer system. A Nicolet-Siemens P3 package was used for data collection and the SHELXTL PLUS software package<sup>15</sup> was used for structure solution and refinement of the data.

<sup>†</sup> Aluminium Carboxylates in Aqueous Solutions. Part 4.<sup>1</sup>

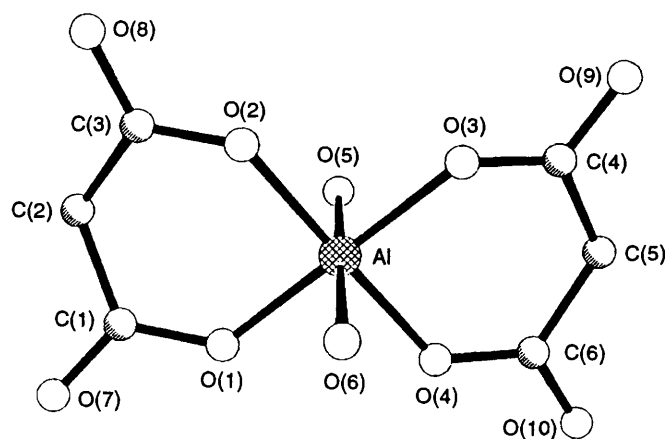


Fig. 1 A view of the  $[\text{Al}(\text{mal})_2(\text{H}_2\text{O})_2]^-$  anion

**Crystal data.**  $\text{C}_6\text{H}_{12}\text{AlKO}_{12}$ ,  $M = 342.2$ , monoclinic, space group  $P2_1/n$ ,  $a = 10.451(3)$ ,  $b = 9.797(3)$ ,  $c = 13.605(3)$  Å,  $\beta = 101.29(2)^\circ$ ,  $U = 1366.0(7)$  Å<sup>3</sup>,  $Z = 4$ ,  $D_c = 1.664$  g cm<sup>-3</sup>,  $\lambda = 0.71073$  Å for Mo-K $\alpha$  radiation,  $F(000) = 704$ ,  $\mu = 0.502$  mm<sup>-1</sup>.

**Data collection and reduction.** The data were collected at 22 °C using the  $\omega$ -scan technique with a  $2\theta$  range of 2.0–50.0°. Scans were made at a variable speed of 1.5–14.65° min<sup>-1</sup> and collected in the index ranges  $h$  0–12,  $k$  0–11 and  $l$  –16 to 15. Of the 2736 reflections collected 2426 were unique ( $R_{\text{int}} = 0.0203$ ). A semiempirical absorption correction was applied with minimum and maximum transmission factors of 0.212 and 0.233.

**Structure solution and refinement.** The structure was solved using direct methods. The non-hydrogen atoms were refined anisotropically. Hydrogen atoms were placed in calculated positions with fixed isotropic  $U$  values. The final cycle of full-matrix least-squares refinement was based on 2231 observed reflections [ $F > 4.0\sigma(F)$ ] and 181 parameters and converged (largest parameter shift 0.001 times its estimated standard deviation, e.s.d.) with unweighted and weighted agreement factors of  $R = 0.0442$  and  $R' = 0.0611$ , where  $w = 1/[\sigma^2(F) + |gF|^2]$ ,  $R' = \Sigma \Delta w^{\frac{1}{2}} / \Sigma w^{\frac{1}{2}} F_o$  and  $g = 0.006$ . The maximum and minimum peaks on the final Fourier-difference map corresponded to 0.60 and –0.50 e Å<sup>-3</sup>, respectively.

Complete atomic coordinates, thermal parameters and bond lengths and angles have been deposited at the Cambridge Crystallographic Data Centre. See Instructions for Authors, *J. Chem. Soc., Dalton Trans.*, 1996, Issue 1.

## Results and Discussion

### Solid-state studies

**Crystal structure.** Atomic coordinates of  $\text{K}[\text{Al}(\text{mal})_2(\text{H}_2\text{O})_2] \cdot 2\text{H}_2\text{O}$  are given in Table 1 and selected bond lengths and angles in Table 2. The structure of the anion is shown in Fig. 1. The  $[\text{Al}(\text{mal})_2(\text{H}_2\text{O})_2]^-$  anion possesses a local mirror symmetry about the O(6)–Al–O(5) plane which is not a crystallographic requirement. The aluminium is six-co-ordinate in an essentially octahedral environment with bond angles ranging from 86.3(1) [O(2)–Al–O(3)] to 93.1(1)° [O(1)–Al–O(2)]. The donors comprise two co-ordinated water molecules O(5) and O(6) which lie *trans* to each other and two bidentate malonate ligands co-ordinating through their carboxylate oxygens O(1), O(2), O(3) and O(4). The bite angles of the malonate ligands are 93.1(1)° [O(1)–Al–O(2)] and 92.1(1)° [O(3)–Al–O(4)] and are significantly greater than

Table 1 Atomic coordinates ( $\times 10^4$ ) for  $\text{K}[\text{Al}(\text{mal})_2(\text{H}_2\text{O})_2] \cdot 2\text{H}_2\text{O}$

Atom	<i>x</i>	<i>y</i>	<i>z</i>
K	6625(1)	2132(1)	5271(1)
Al	4895(1)	2483(1)	2635(1)
O(1)	5467(2)	832(2)	3256(1)
O(2)	3299(2)	1746(2)	1990(1)
O(3)	4304(2)	4124(2)	2018(1)
O(4)	6465(2)	3281(2)	3289(1)
O(5)	5676(2)	2060(2)	1515(1)
O(6)	4191(2)	2889(2)	3795(1)
O(7)	5371(2)	–1339(2)	3649(2)
O(8)	1978(2)	224(2)	1168(2)
O(9)	4475(2)	6016(2)	1200(2)
O(10)	8070(2)	4745(2)	3606(2)
C(1)	4967(2)	–361(3)	3100(2)
C(2)	3896(3)	–632(3)	2198(2)
C(3)	2996(2)	503(3)	1762(2)
C(4)	4946(3)	5150(3)	1830(2)
C(5)	6305(4)	5377(5)	2344(4)
C(6)	6988(2)	4407(3)	3138(2)
O(11)	9115(2)	2614(2)	4792(1)
O(12)	6877(2)	–761(2)	5469(2)

Table 2 Selected bond lengths (Å) and angles (°) for  $\text{K}[\text{Al}(\text{mal})_2(\text{H}_2\text{O})_2] \cdot 2\text{H}_2\text{O}$

Al–O(1)	1.868(2)	O(4)–C(6)	1.265(3)
Al–O(2)	1.871(2)	O(7)–C(1)	1.237(3)
Al–O(3)	1.862(2)	O(8)–C(3)	1.234(3)
Al–O(4)	1.877(2)	O(9)–C(4)	1.238(3)
Al–O(5)	1.909(2)	O(10)–C(6)	1.229(3)
Al–O(6)	1.909(2)	C(1)–C(2)	1.514(4)
O(1)–C(1)	1.281(3)	C(7)–C(3)	1.501(4)
O(2)–C(3)	1.281(3)	C(4)–C(5)	1.472(5)
O(3)–C(4)	1.262(3)	C(5)–C(6)	1.510(5)
O(1)–Al–O(2)	93.1(1)	Al–O(3)–C(4)	129.5(2)
O(1)–Al–O(3)	179.3(1)	Al–O(4)–C(6)	130.6(2)
O(2)–Al–O(3)	86.3(1)	O(1)–C(1)–O(7)	121.8(2)
O(1)–Al–O(4)	88.5(1)	O(1)–C(1)–C(2)	120.5(2)
O(2)–Al–O(4)	177.9(1)	O(7)–C(1)–C(2)	117.7(2)
O(3)–Al–O(4)	92.1(1)	C(1)–C(2)–C(3)	119.8(2)
O(1)–Al–O(5)	91.4(1)	O(2)–C(3)–O(8)	120.7(2)
O(2)–Al–O(5)	91.3(1)	O(2)–C(3)–C(2)	120.1(2)
O(3)–Al–O(5)	89.1(1)	O(8)–C(3)–C(2)	119.2(2)
O(4)–Al–O(5)	89.9(1)	O(3)–C(4)–O(9)	122.1(2)
O(1)–Al–O(6)	87.0(1)	O(3)–C(4)–C(5)	121.7(3)
O(2)–Al–O(6)	90.9(1)	O(9)–C(4)–C(5)	116.2(3)
O(3)–Al–O(6)	92.6(1)	C(4)–C(5)–C(6)	121.5(3)
O(4)–Al–O(6)	87.9(1)	O(4)–C(6)–O(10)	122.3(2)
O(5)–Al–O(6)	177.3(1)	O(4)–C(6)–C(5)	120.4(2)
Al–O(1)–C(1)	129.1(1)	O(10)–C(6)–C(5)	117.3(3)
Al–O(2)–C(3)	129.5(2)		

those found in the  $[\text{Fe}(\text{mal})_3]^{3-}$  complex<sup>16</sup> which range from 86.8(1) to 88.6(1)°. The Al–O bond lengths for the ligands range from 1.862(2) to 1.877(2) Å with each ligand having one shorter and one longer interaction. These are shorter than those found in  $[\text{Fe}(\text{mal})_3]^{3-}$  [1.962(1)–2.022(1) Å] as would be expected for the smaller Al<sup>3+</sup> ion. A comparison of the distance between the two chelating oxygens of the ligand in both complexes shows that again they are shorter in  $[\text{Al}(\text{mal})_2(\text{H}_2\text{O})_2]^-$  with an average of 2.70 Å as compared with the average of 2.76 Å for  $[\text{Fe}(\text{mal})_3]^{3-}$ . This illustrates that the bite of the bidentate malonate ligand is reduced in  $[\text{Fe}(\text{mal})_3]^{3-}$  as would be expected from the fact that the *trans*-co-ordinated water molecules enforce different ligation of the malonate.

The anions are connected to each other in the crystal structure by a complicated network formed by interactions of the potassium counter ions with the crystal waters and the oxygens of the co-ordinated waters and malonate carboxylate oxygens such that each K<sup>+</sup> ion is eight-co-ordinate.

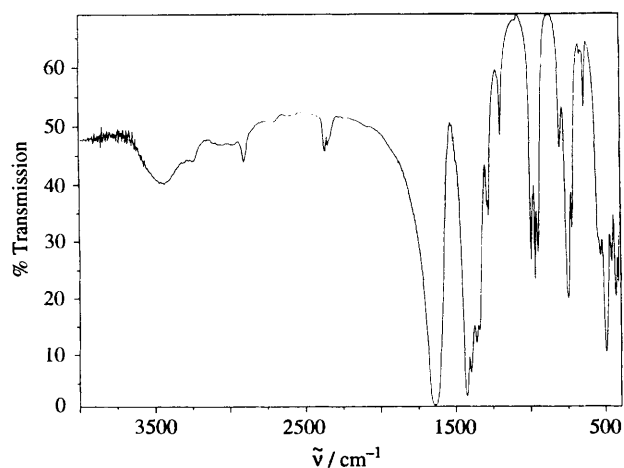


Fig. 2 The Fourier-transform IR spectrum of the complex  $\text{K}[\text{Al}(\text{mal})_2(\text{H}_2\text{O})_2] \cdot 2\text{H}_2\text{O}$  (1% in KBr)

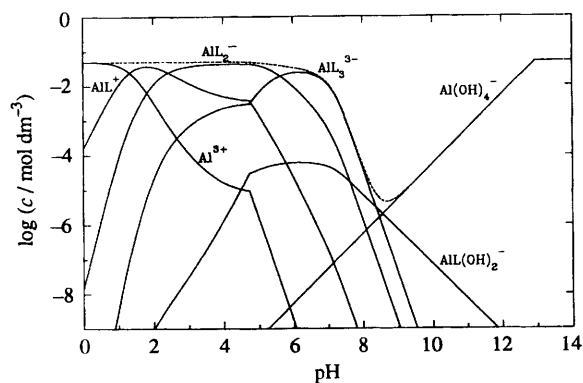


Fig. 3 Species distribution diagram for a  $50 \text{ mmol dm}^{-3}$  solution of  $\text{K}[\text{Al}(\text{mal})_2(\text{H}_2\text{O})_2] \cdot 2\text{H}_2\text{O}$ . All thermodynamic data from ref. 10 have been used but most hydroxoaluminium complexes are not shown

**IR Spectroscopy.** The solid-state IR spectrum of  $\text{K}[\text{Al}(\text{mal})_2(\text{H}_2\text{O})_2] \cdot 2\text{H}_2\text{O}$  (1% in KBr) is shown in Fig. 2. The bands at  $1636$  and  $1422 \text{ cm}^{-1}$  can be assigned to the  $\nu_{\text{asym}}(\text{CO}_2)$  and  $\nu_{\text{sym}}(\text{CO}_2)$  stretches of the carboxylate groups. These have a  $\Delta\nu(\text{CO}_2)$  value of  $214 \text{ cm}^{-1}$  which fits with an 'ester like' co-ordination mode, according to the criterion of Deacon and Phillips.<sup>17</sup>

#### Solution-state studies

**Potentiometric titrations.** Thermodynamic predictions for the  $\text{Al}^{\text{III}}\text{-H}_2\text{mal}\text{-water}$  system are shown in the species distribution diagram (Fig. 3), obtained on the basis of the available data.<sup>10</sup> It shows that the complex  $[\text{Al}(\text{mal})_2(\text{H}_2\text{O})_2]^-$  is expected to be the dominant species within a significant pH range in the acid region ( $3 < \text{pH} < 5.5$ ). From  $\text{pH} \text{ ca. } 5$  its gradual decomposition into aluminium hydroxide and  $[\text{Al}(\text{mal})_3]^{3-}$  is predicted.

**NMR Spectroscopy.** Dissolution of the complex  $\text{K}[\text{Al}(\text{mal})_2(\text{H}_2\text{O})_2] \cdot 2\text{H}_2\text{O}$  to give a  $50 \text{ mmol dm}^{-3}$  solution in  $\text{D}_2\text{O}$  is accompanied by a slight pD change (from 7.50 to 6.36) but no precipitate was observed. On changing the pD of these solutions precipitation of aluminium hydroxide occurred only for  $\text{pD} \geq 8.0$ .

The  $^1\text{H}$  NMR spectrum of a  $50 \text{ mmol dm}^{-3}$  solution of malonate at pD 7.40 displays a rather composite signal centred at  $\delta 3.11$  [Fig. 4(a)]. The multiplicity of the signal is attributed to H/D exchange of the intercarboxylate methylene group<sup>13</sup> which results in scalar coupling between  $^1\text{H}$  ( $I = \frac{1}{2}$ ) and  $^2\text{D}$  ( $I = 1$ ) nuclei. A similar observation is made in the  $^{13}\text{C}$  NMR

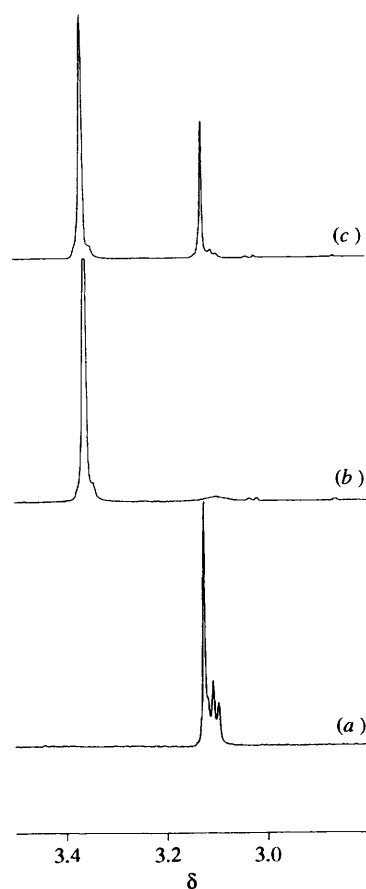


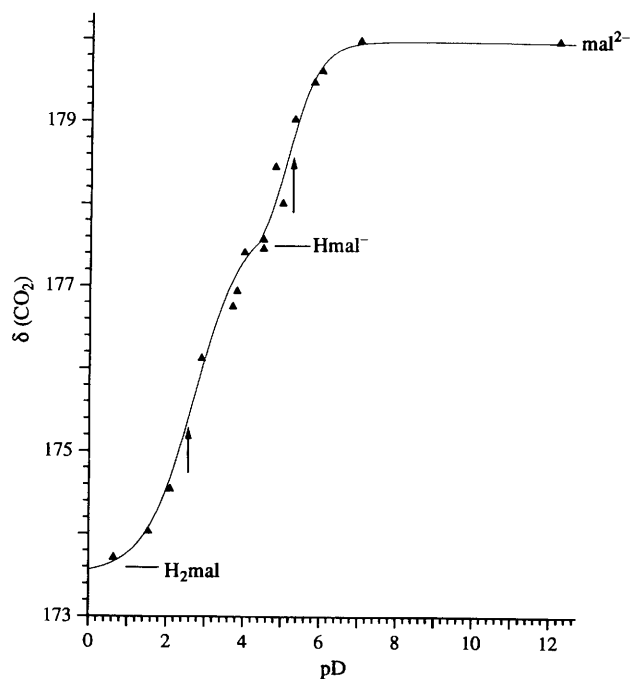
Fig. 4 The  $400 \text{ MHz } ^1\text{H}$  NMR spectra in  $\text{D}_2\text{O}$  of:  $50 \text{ mmol dm}^{-3}$  solutions of (a) malonic acid at pD 7.40; (b)  $\text{K}[\text{Al}(\text{mal})_2(\text{H}_2\text{O})_2] \cdot 2\text{H}_2\text{O}$  at pD 7.39 and (c) malonic acid and  $\text{K}[\text{Al}(\text{mal})_2(\text{H}_2\text{O})_2] \cdot 2\text{H}_2\text{O}$  at pD 7.38

( $^{13}\text{C}$ ,  $I = \frac{1}{2}$ ) spectrum of malonic acid where the signal of the aliphatic carbon ( $\text{CH}_2$ ) shows  $^{13}\text{C}\text{-}^2\text{D}$  coupling (see later). In Fig. 4(b) the spectrum of a  $50 \text{ mmol dm}^{-3}$  solution of redissolved  $\text{K}[\text{Al}(\text{mal})_2(\text{H}_2\text{O})_2] \cdot 2\text{H}_2\text{O}$ , pD 7.39, is shown. It is characterized by a signal at  $\delta 3.36$  which has a shoulder to high field, indicating some H/D exchange has occurred. There was no change in this spectrum on changing the pD (from 6.4 to 7.4) following dissolution of the crystals. On addition of  $50 \text{ mmol dm}^{-3}$  malonic acid [Fig. 4(c)] an additional signal is seen at  $\delta 3.1$  which is identical to that observed for free malonic acid. Comparing the spectra in Fig. 4 one can conclude that the signal at  $\delta 3.36$  is from a malonate complex and that on redissolving  $\text{K}[\text{Al}(\text{mal})_2(\text{H}_2\text{O})_2] \cdot 2\text{H}_2\text{O}$  in  $\text{D}_2\text{O}$  any hydrolysis reactions that occur do not result in the formation of a significant amount of uncomplexed malonate.

The  $^{13}\text{C}\text{-}\{^1\text{H}\}$  NMR spectrum for a solution of  $150 \text{ mmol dm}^{-3}$  malonic acid at pD 5.8 is characterized by a singlet at  $\delta 179.4$  and a set of signals between  $\delta 48$  and  $49$ , from the  $\text{CO}_2$  and  $\text{CH}_2$  groups, respectively. In an analogous manner to the  $^1\text{H}$  NMR spectrum a splitting pattern is observed for the aliphatic carbon due to  $^{13}\text{C}\text{-}^2\text{D}$  scalar coupling. The H/D exchange appeared to be dependent on a number of factors including the pD and the metal-to-ligand ratio and this complication made a comparison of the aliphatic regions of the  $^{13}\text{C}$  NMR spectra of different  $\text{Al}^{3+}\text{-malonate}$  solutions not informative as far as characterizing the speciation profiles. The chemical shifts of these two signals are pH dependent, as shown in Fig. 5, allowing the chemical shifts of the  $\text{H}_2\text{mal}$ ,  $\text{Hmal}^-$  and  $\text{mal}^{2-}$  species to be determined (Table 3). The  $\text{p}K_a$  values can also be determined and compare very well with those previously obtained from potentiometry<sup>10</sup> (Table 4). The  $^{13}\text{C}$  NMR spectrum for a  $50 \text{ mmol dm}^{-3}$  solution of  $[\text{Al}(\text{mal})_2(\text{H}_2\text{O})_2]^-$  at

**Table 3** Carbon-13 NMR chemical shifts ( $\delta$ ) for the  $\text{Al}^{3+}$ -malonate system

Group	Species			$[\text{Al}(\text{mal})_2]^-$		$[\text{Al}(\text{mal})_3]^{3-}$	
	$\text{H}_2\text{mal}$	$\text{Hmal}^-$	$\text{mal}^{2-}$	pD 5.9	pD 7.5	pD 5.9	pD 7
$\text{CH}_2$	43.8	44.4	50.2	44.2		44.4	
$\text{CO}_2$	173.8	177.8	180.0	177.5	177.6	177.9	178.0

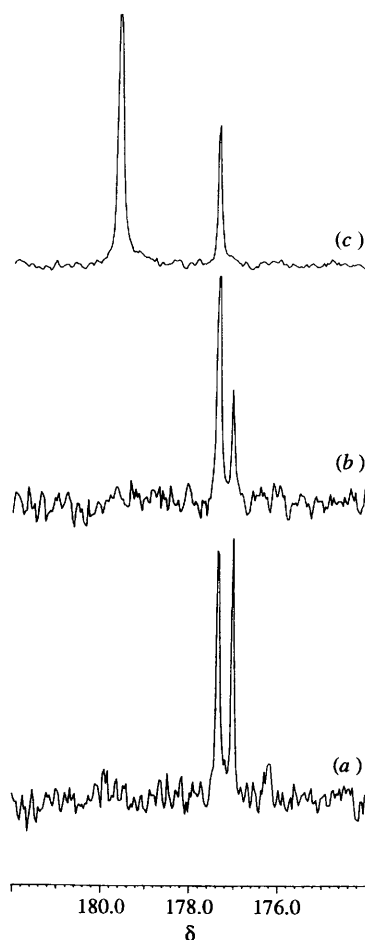
**Fig. 5** Effect of pH on the  $^{13}\text{C}$  NMR chemical shift for the carboxylate signal of free malonic acid. Vertical arrows represent  $\text{p}K_a$  values determined by potentiometry. Curve fitting by two single exponential processes gave pD values of 2.73 and 5.13

autogenous pD (=6.4) is shown in Fig. 6(a). In the region associated with the carboxylate resonances two well separated signals with approximately equal intensity are observed at  $\delta$  178.0 and 177.6. These signals are likely to be from malonate complexes as the chemical shift for free malonate (*i.e.* not complexed by  $\text{Al}^{3+}$ ) at this pD is  $\delta$  180.0 (see Fig. 5). On changing the pD to 7.4 the relative intensity of the two signals changes with that at  $\delta$  178.0 dominating the one at  $\delta$  177.6 [Fig. 6(b)]. This is consistent with the assignment of the signals to two different complexes as opposed to two different signals from the same complex. The effect of the addition of 500  $\text{mmol dm}^{-3}$  malonic acid to the solution is shown in Fig. 6(c). Two signals are observed, one at  $\delta$  178.0, as before, and a new one at  $\delta$  180.0. This latter signal was assigned to free malonic acid, as malonic acid at pD 7.4 in the absence of  $\text{Al}^{3+}$  has the same  $\delta$ . The large excess of malonic acid used will quantitatively convert  $[\text{Al}(\text{mal})_2(\text{H}_2\text{O})_2]^-$  into  $[\text{Al}(\text{mal})_3]^{3-}$  allowing the two signals from the malonate complexes to be assigned as  $[\text{Al}(\text{mal})_3]^{3-}$  at  $\delta$  178.0 and  $[\text{Al}(\text{mal})_2(\text{H}_2\text{O})_2]^-$  at  $\delta$  177.6 (Table 3).

The  $^{27}\text{Al}$  NMR spectrum of a 50  $\text{mmol dm}^{-3}$   $\text{K}[\text{Al}(\text{mal})_2(\text{H}_2\text{O})_2] \cdot 2\text{H}_2\text{O}$  solution is uncomplicated showing a single relatively sharp signal at  $\delta$  2.5 indicating aluminium in an octahedral environment co-ordinated by six oxygen atoms.<sup>18,19</sup> The signal is temperature dependent with a reduction in peak width at elevated temperature (up to 70 °C) and no additional signals are observed. Changing the pD over the range 3.5–7.5 has no effect on the signal (Fig. 7). This could indicate that  $[\text{Al}(\text{mal})_2(\text{H}_2\text{O})_2]^-$  is stable in solution, contrary to the distribution profile, or alternatively that  $^{27}\text{Al}$  NMR spectro-

**Table 4** Comparison of the  $\text{p}K_a$  values for malonic acid ( $\text{H}_2\text{L}$ ) determined from potentiometric titrations and  $^{13}\text{C}$  NMR spectroscopy

Method	$\text{p}K_a$	
	$\text{H}_2\text{L}$	HL
Potentiometry	2.59	5.15
$^{13}\text{C}$ NMR	2.73	5.13

**Fig. 6** The 100.4 MHz  $^{13}\text{C}$  NMR spectra in  $\text{D}_2\text{O}$  for a 50  $\text{mmol dm}^{-3}$  solution of  $\text{K}[\text{Al}(\text{mal})_2(\text{H}_2\text{O})_2] \cdot 2\text{H}_2\text{O}$ : (a) at autogenous pH (pD 6.36); (b) at neutral pH (pD 7.40) and (c) with an excess (500  $\text{mmol dm}^{-3}$ ) of malonic acid at pD 7.42. 3000 Transients collected using a 8  $\mu\text{s}$  pulse and a recycle time of 4.34 s

scopy cannot resolve signals from the  $[\text{Al}(\text{mal})_2(\text{H}_2\text{O})_2]^-$  and  $[\text{Al}(\text{mal})_3]^{3-}$  complexes.

This situation can be clarified by the parallel use of  $^{13}\text{C}$  and  $^{27}\text{Al}$  NMR spectroscopy. The  $^{27}\text{Al}$  NMR spectrum of a 1:2  $\text{Al}^{3+}$ -malonate solution [50  $\text{mmol dm}^{-3}$   $\text{Al}(\text{NO}_3)_3 \cdot 9\text{H}_2\text{O}$ , 100  $\text{mmol dm}^{-3}$  malonic acid, pD 5.9], Fig. 8(a)(i), is identical to that of the solution of redissolved  $\text{K}[\text{Al}(\text{mal})_2(\text{H}_2\text{O})_2] \cdot 2\text{H}_2\text{O}$ . The  $^{13}\text{C}$  NMR spectrum [Fig. 8(b)(i)] shows two signals in the carboxylate region with the low-field signal assigned to

the  $[\text{Al}(\text{mal})_3]^{3-}$  complex and the high-field signal to  $[\text{Al}(\text{mal})_2(\text{H}_2\text{O})_2]^-$  as outlined earlier; the chemical shift for free malonate at this pD is  $\delta$  179.3 (see Fig. 5). The distribution diagram (Fig. 3) indicates these will be the two major malonate complexes under the conditions. The  $^{27}\text{Al}$  NMR spectrum of the corresponding 1 : 3  $\text{Al}^{3+}$ -malonate solution at the same pD is identical to that of the 1 : 2 solution [compare Fig. 8(a)(i) and (a)(ii)]. However, the  $^{13}\text{C}$  NMR spectrum is different with the two signals observed in the carboxylate region assigned to free malonic acid and  $[\text{Al}(\text{mal})_3]^{3-}$  on the basis of their chemical shifts [compare Fig. 8(b)(i) and (b)(ii)]. This shows that although both the  $[\text{Al}(\text{mal})_2(\text{H}_2\text{O})_2]^-$  and  $[\text{Al}(\text{mal})_3]^{3-}$  complexes can coexist in solution it is not possible to resolve different resonances for them by  $^{27}\text{Al}$  NMR spectroscopy. This

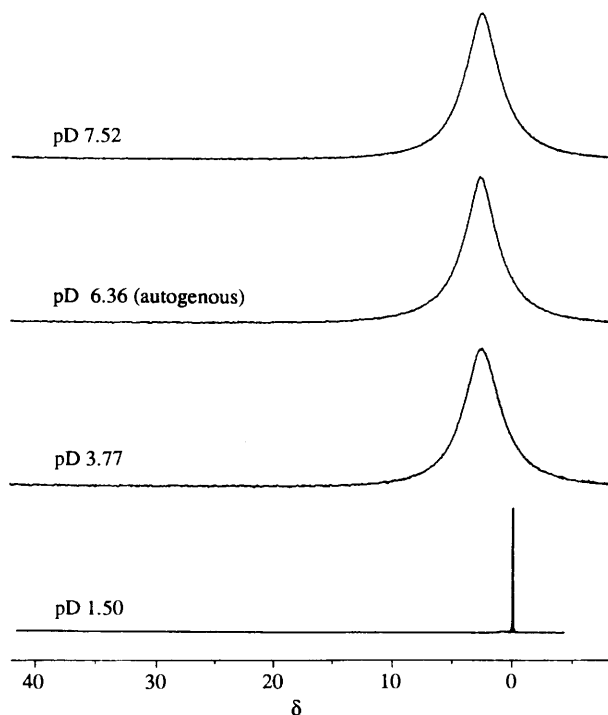


Fig. 7 The 104.5 MHz  $^{27}\text{Al}$  NMR spectra for a 50 mmol  $\text{dm}^{-3}$  solution in  $\text{D}_2\text{O}$  of  $\text{K}[\text{Al}(\text{mal})_2(\text{H}_2\text{O})_2]\cdot 2\text{H}_2\text{O}$  at several pD. 1024 Transients collected using a 10  $\mu\text{s}$  pulse and a recycle time of 0.56 s

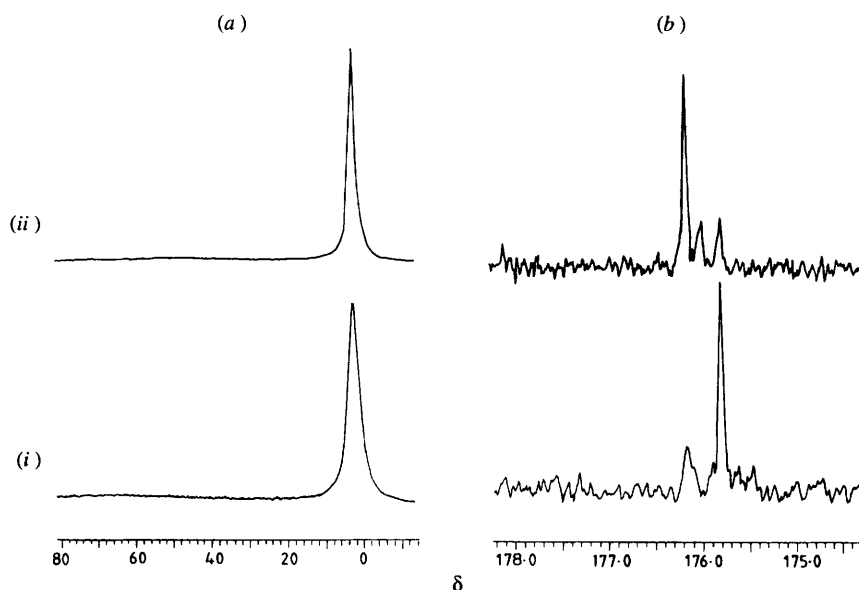


Fig. 8 The 104.5 MHz  $^{27}\text{Al}$  NMR spectra, 1024 transients collected using a 10  $\mu\text{s}$  pulse and a recycle time of 0.56 s (a) and 100.4 MHz  $^{13}\text{C}$  NMR spectra, 3000 transients collected using a 8  $\mu\text{s}$  pulse and a recycle time of 4.34 s (b), in  $\text{D}_2\text{O}$  of (i) 50 mmol  $\text{dm}^{-3}$   $\text{Al}(\text{NO}_3)_3\cdot 9\text{H}_2\text{O}$  + 100 mmol  $\text{dm}^{-3}$  malonic acid, pD 5.9, (ii) 50 mmol  $\text{dm}^{-3}$   $\text{Al}(\text{NO}_3)_3\cdot 9\text{H}_2\text{O}$  + 150 mmol  $\text{dm}^{-3}$  malonic acid, pD 5.9

is perhaps not surprising in view of the similar co-ordination environments of the  $\text{Al}^{3+}$ .

It is worth noting that in the solid-state structure of  $\text{K}[\text{Al}(\text{mal})_2(\text{H}_2\text{O})_2]\cdot 2\text{H}_2\text{O}$  the two malonate ligands are *cis* to one another forming a planar arrangement and the two waters are *trans* to each other. Conversion of this complex into  $[\text{Al}(\text{mal})_3]^{3-}$  [equation (1), where  $m + n = 6$ ] would involve



ligand rearrangement so that the two water co-ordination sites lie *cis* to one another allowing the third malonate ligand to co-ordinate. In solution the different isomers of  $[\text{Al}(\text{mal})_2(\text{H}_2\text{O})_2]^-$  will interchange and because they are very similar they are unlikely to be resolved by NMR spectroscopy.

On the basis of the above measurements the solution state of  $\text{K}[\text{Al}(\text{mal})_2(\text{H}_2\text{O})_2]\cdot 2\text{H}_2\text{O}$  can be depicted in the following terms. When the complex is dissolved in neutral  $\text{D}_2\text{O}$  it undergoes partial hydrolysis to give  $[\text{Al}(\text{mal})_3]^{3-}$ , which is thermodynamically more stable, and non-detectable aquahydroxo species. The alternative of disproportionation to give  $[\text{Al}(\text{mal})]^{+}$ ,  $[\text{Al}(\text{mal})_2]^{-}$  and  $[\text{Al}(\text{mal})_3]^{3-}$  can be ruled out by the  $^{13}\text{C}$  NMR studies (Fig. 6) and the distribution diagram (Fig. 3). Hydrolysis of the bis complex,  $[\text{Al}(\text{mal})_2]^{-}$ , is favoured when the pH of the solution is raised (from pD 6.4 to 7.4) and the tris complex,  $[\text{Al}(\text{mal})_3]^{3-}$ , becomes the main species in neutral solution. Moreover, excess of malonic acid quantitatively converts  $[\text{Al}(\text{mal})_2(\text{H}_2\text{O})_2]^-$  into  $[\text{Al}(\text{mal})_3]^{3-}$ .

This interpretation fits with the  $^1\text{H}$  NMR pattern if one accepts that hydrolysis of the bis complex ( $\delta$  3.36) is limited to the extent required for conversion of the remainder of the bis complex into  $[\text{Al}(\text{mal})_3]^{3-}$  and there is no significant formation of free malonic acid. Thus two thirds of the  $\text{Al}^{3+}$  remains bound to mal and one third forms an aquahydroxo compound. The overlap of proton resonances for the malonate ligand in the bis and tris complexes would have made these conclusions impossible to substantiate in the absence of the  $^{13}\text{C}$  NMR data where signals from the two complexes can be resolved. The inability to detect the aquahydroxo aluminium species by  $^{27}\text{Al}$  NMR spectroscopy is not surprising as any signal from a monomeric species will overlap that of the aluminium malonate complexes, since they have the same donor set, and the low symmetry of a polymeric species will lead

to a very broad signal non-resolvable from the baseline.<sup>18-20</sup>

As a final observation, it is worth noting that for an aluminium concentration of 50 mmol dm<sup>-3</sup> the observed dominating species in neutral solutions, [Al(mal)<sub>3</sub>]<sup>3-</sup>, is metastable, *i.e.* resistant to the predicted conversion into Al(OH)<sub>3</sub>.

### Acknowledgements

We are grateful to the European Science Foundation for the provision of a fellowship allowing A. T. to begin a useful collaboration with U.E.A, School of Chemical Sciences, where most of this work has been carried out. We are indebted to Dr. R. Bertani for kind assistance in the NMR measurements and Professors B. Corain and G. G. Bombi for helpful discussions.

### References

- 1 Part 3, A. A. Sheikh-Osman, R. Bertani, A. Tapparo, G. G. Bombi and B. Corain, *J. Chem. Soc., Dalton Trans.*, 1993, 3229.
- 2 J. A. Sturman and Wisniewski, in *Metal Neurotoxicity*, eds. S. C. Bondy and K. N. Prasad, CRC Press, Boca Raton, FL, 1988, p. 61.
- 3 D. R. Crapper McLachlan, *Neurobiol. Aging*, 1986, 7, 525.
- 4 D. R. Crapper McLachlan, W. J. Lukiw and T. P. A. Kruck, *Environ. Geochem. Health*, 1990, 12, 103.
- 5 A. C. Alfrey, in *Aluminium in Chemistry, Biology and Medicine*, eds. M. Nicolini, P. Zatta and B. Corain, Cortina International-Raven Press, Verona, 1991, p. 73.
- 6 K. Abreo, S. T. Brown and M. Less Sella, *Am. J. Kidney Dis.*, 1989, 13, 465.
- 7 B. Corain, A. Tapparo, A. A. Sheikh-Osman, G. G. Bombi, P. Zatta and M. Favaro, *Coord. Chem. Rev.*, 1992, 112, 19.
- 8 G. G. Bombi, B. Corain, A. A. Sheikh-Osman and G. C. Valle, *Inorg. Chim. Acta*, 1990, 171, 79.
- 9 B. Corain, B. Longato, A. A. Sheikh-Osman, G. G. Bombi and C. Maccà, *J. Chem. Soc., Dalton Trans.*, 1992, 169.
- 10 T. Kiss, I. Sóvágó, R. B. Martin and J. Pursiainen, *J. Inorg. Biochem.*, 1994, 55, 53.
- 11 F. T. Greenaway, *Inorg. Chim. Acta*, 1986, 116, L21.
- 12 F. R. Venema, J. A. Peters and H. van Bekkum, *J. Chem. Soc., Dalton Trans.*, 1990, 2137.
- 13 S. Amirhaeri, M. E. Farago, J. A. P. Gluck, M. A. R. Smith and J. N. Wingfield, *Inorg. Chim. Acta*, 1979, 33, 57.
- 14 A. K. Covington, M. Paabo, R. A. Robinson and R. G. Bates, *Anal. Chem.*, 1968, 40, 700.
- 15 G. M. Sheldrick, SHELXTL PLUS, Siemens Analytical Instruments, Madison, WI, 1990.
- 16 W. Clegg, *Acta Crystallogr., Sect. C*, 1985, 41, 1164.
- 17 G. B. Deacon and R. J. Phillips, *Coord. Chem. Rev.*, 1980, 33, 227.
- 18 J. W. Akitt, *Prog. Nucl. Magn. Reson. Spectrosc.*, 1989, 21, 1.
- 19 P. A. Jordan, N. J. Clayden, S. L. Heath, G. R. Moore, A. K. Powell and A. Tapparo, *Coord. Chem. Rev.*, 1996, in the press.
- 20 J. W. Akitt, J. M. Elders, X. L. R. Fontaine and A. K. Kundu, *J. Chem. Soc., Dalton Trans.*, 1989, 1897.

Received 16th August 1995; Paper 5/05474E